Thermal Conductivity of Zincblende Crystals

Amelia Carolina Sparavigna[1]

1 – Department of Applied Science and Technology, Politecnico di Torino, Torino, Italy

Keywords: thermal conductivity, phonons, Boltzmann equation

ABSTRACT. Among materials having zincblende lattices, we find some that are characterized by a high thermal conductivity. This is a quite important feature for their application in semiconductor technologies and related devices. In this paper, we will discuss the thermal conductivity of two zincblende crystals (SiC and GaAs), stressing the role of lattice vibrations in producing high values of conductivity and of lattice defects in reducing it. In the framework of a model dealing with phonon dispersions and reliable scattering mechanisms, we will show how lattice thermal conductivity can be estimated from the Boltzmann Transport Equation in the case of any zincblende crystal.

Introduction. Measurements of thermal conductivities reveal that most of the high thermal conductors are adamantine (diamond-like) solids: among them we have Diamond, SiC, AlN, GaN and Si [1,2]. For instance, the silicon carbide (SiC), a material which is fundamental for semiconductor technologies and for future innovations of them [3-5], has at room temperature a conductivity greater than 3 $W\ cm^{-1}K^{-1}$ in the CVD grade and about 1 $W\ cm^{-1}K^{-1}$ when sintered [6,7]. Such a high thermal conductivity could be surprising, because it is commonly believed that it is possessed just by metals, due to the presence in them of a free flowing cloud of electrons. In non-metallic solids, electrons are not free to move and therefore phonons are the only responsible for heat transport. They are so efficient, that in the diamond at room temperature they are producing an intrinsic thermal conductivity much higher than that measured in metals. Aluminium for instance has conductivity of about 2 $W\ cm^{-1}K^{-1}$ [8], whereas natural diamond has a conductivity of about 20 $W\ cm^{-1}K^{-1}$ at room temperature.

Compounds consisting of more than one element have often a crystal structure based on the cubic crystal system of the zincblende type. This crystal is like an adamantine lattice where two atom types form two interpenetrating face-centred cubic lattices. The zincblende structure has a tetrahedral coordination: each atom's nearest neighbours consist of four atoms of the opposite type, positioned like the four vertices of a regular tetrahedron. So the arrangement of atoms is the same as a diamond cubic structure, but with alternating types of atoms at the different lattice sites. Examples of compounds with this structure include gallium arsenide, boron arsenide (shown in the Figure 1), cadmium telluride and a wide assembly of other binary compounds.

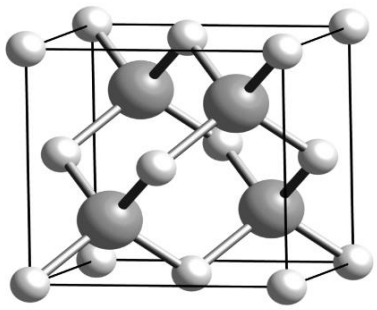

Figure 1. The lattice cell of Born Arsenide in the zincblende structure (Courtesy Wikipedia)

Some materials, such as abovementioned SiC and AlN ceramics for instance, are fundamental for the development of new devices including light emitting diode (LED) [9-11]. Since in these devices the dissipation of heat is crucial, it is important investigating their thermal conductivity and how disorder produced by point and extended defects can influence their thermal transport. For instance in diamond, the isotope disorder alone is able to strongly reduce thermal conductivity, even at room temperature [12]. And also experimental data for Silicon indicate a large rise in the thermal conductivity of isotopically pure Si when compared to natural Si [13-15].

Let us therefore discuss the thermal transport properties of zincblende crystals, in particular SiC and GaAs. We will propose for them a calculus of phononic thermal conductivity in the framework of an iterative approach used for diamond-like lattice [16-17]. In fact, this calculation can be easily applied to any other zincblende lattice, if we have phononic dispersion curves and dielectric constants for fitting parameters used in the calculation.

2. Importance of SiC and GaAs. Among adamantine compounds, Silicon Carbide and Gallium Arsenide are fundamental for electronic and optical applications: the first because it is able dissipating heat in devices, the second because components and integrated circuits obtained with this material are faster than those made of silicon, due to a large low-field electron mobility. GaAs compound is able to emit light, turning out to be useful for making lasers and light-emitting diodes in devices where the material is subjected to very high thermal gradients [11]. Silicon Carbide is an excellent abrasive and for this reason it had been produced for abrasive products under the name of Carborundum [18]. However, today, best applications of this material are in those devices where its high thermal conductivity coupled with a high strength allows enduring large thermal shocks. In this manner, SiC is very popular as wafer tray supports in semiconductor furnaces [19].
Silicon Carbide crystallizes in several polytypes; the two most common SiC polytypes are 3C-SiC and 6H-SiC. 3C polytype, also known as beta-SiC, is the only polytype with a cubic structure. In addition to 3C-SiC, several hexagonal and rhombohedral lattice SiC crystal structure arrangements are possible. They are known as alpha-SiC. 3C-SiC crystallizes is a zincblende structure, hence it can be deposited on Si [20]. Compared to Si, SiC exhibits a larger band-gap, a higher breakdown field, a higher thermal conductivity and a high saturation velocity (see Table 1, [20,21]). These properties make SiC very attractive for the fabrication of high temperature, high-power and high frequency electronic devices. In addition, it is a material used for fabrication of microsensors that can operate at high temperatures, for instance, as pressure sensors in engines [22,23]. In comparison to diamond, attractive features of SiC are that it can be doped both p- and n- type and it allows a natural oxide to be grown on its surface.

Table 1. Material Properties of Common Semiconductor Materials at 300K

Property	**3C-SiC (6H-SiC)**	**GaAs**	**Si**	**Diamond**
Melting Point (^{o}C)	Sublimes at 1825	1238	1415	Phase Change
Max. Operating Temp. (^{o}C)	873 (1240)	460	300	1100
Thermal Conductivity (W/cm ^{o}C)	4.9	.5	1.5	20
Energy Gap (eV)	2.2 (2.9)	1.42	1.12	5.5
Dielectric Constant	9.7	13.2	11.9	5.5
Lattice constant (Å)	4.36	5.65	5.43	3.57

Gallium arsenide is used in the manufacture of devices such as microwave frequency integrated circuits and light-emitting diodes [11]. Because the GaAs films are usually epitaxially grown, they are monocrystalline and have atomically flat interfaces. These films are extremely well controlled, unlike polycrystalline materials. With GaAs, lattice mismatches can be easily avoided and then GaAs-based systems, such as InP-based material systems, allow for direct incorporation of optical functions into mechanical structures [11]. Finally, its zincblende structure allows for piezoelectricity as a result of lack of center of symmetry, in contrast to silicon. This property leads to interesting sensing applications (see for instance Ref.24). Another advantage of GaAs is that it has a direct band gap, which means that it can be used to absorb and emit light efficiently [11].

3. Phononic thermal transport in cubic SiC and GaAs. Let us apply an approach to the evaluation of thermal conductivity in zincblende crystals, which had been developed for diamond structures [16]. In this approach, solids are described by means of a microscopic model considering the discrete nature of lattice, a true Brillouin Zone for phonon dispersions (acoustic and optical) and rigorous phonon scattering mechanisms. The phononic Boltzmann equation is solved avoiding relaxation time approximations, an approximation usually made to describe a phonon collision with other phonons and defects. C, Si and Ge have been investigated [14,16] and the role of isotope effects on thermal conductivity deeply discussed, finding good agreement with experimental data.

Let us consider a phonon system of a solid with a diamond-like lattice, with two atoms in the cell basis, but with different masses, as in the case of Figure 1. The model considers a lattice with its cell positions and atomic positions in cell basis. Crystal sites are interacting with a pair potential $V(r)$, where r is the interatomic distance. The potential can then be described in terms of six parameters denoted by ρ, ρ', β, β', ε and ε' whose definitions are given in Ref.16. The parameters ρ, ρ', β, β' are governing the equation of atomic motion and can be obtained by fitting experimental phonon dispersion curves. Parameters ε and ε' are obtained from Grüneisen parameter.

The crystal excitations in the harmonic approximation, that is the phonons, are described by wave-vectors q of the Brillouin Zone, and polarization index p, with a frequency ω_{qp}. The lattice displacement field η is then written in terms of phonon absorption and creation operators a_{qp}, a^{+}_{qp} [25]. After, to obtain phonon frequencies and dispersions, expanding function V in terms of lattice site displacement operator η, we obtain second and third order terms of the potential energy for two interacting atoms at different lattice positions. The pair potential has adjustable parameters used to fit phonon dispersions and Grüneisen parameter [16].

In Figure 2, the phonon dispersions for GaAs are shown in comparison with experimental data (in the same figure, the phonon dispersions for SiC are also given). The theoretical calculation is here performed by means of atomic motion equations, including in phonon Hamiltonian a perturbation term to describe the shift of longitudinal optical LO mode. The perturbation changes LO mode frequencies by a factor $(\varepsilon_0/\varepsilon_\infty)^{1/2}$, as discussed by Born and Huang [25]: ε_0, ε_∞ are static and high frequency dielectric constants respectively. For GaAs, LO mode shift turns out to be about 9% (ε_0=12.9, ε_∞=10.89) [26]. Let us note that the model is able to fit transverse acoustic modes in the main directions of the Brillouin Zone, with an overall good agreement with experimental data from Ref.27. The same approach for LO-mode shift is used for cubic Silicon Carbide too. For SiC, ε_0=9.71, ε_∞=6.52 give a shift of 22%, and the same value results by fitting phonon dispersion data of LO branch (see Fig.2, experimental data from Ref.28).

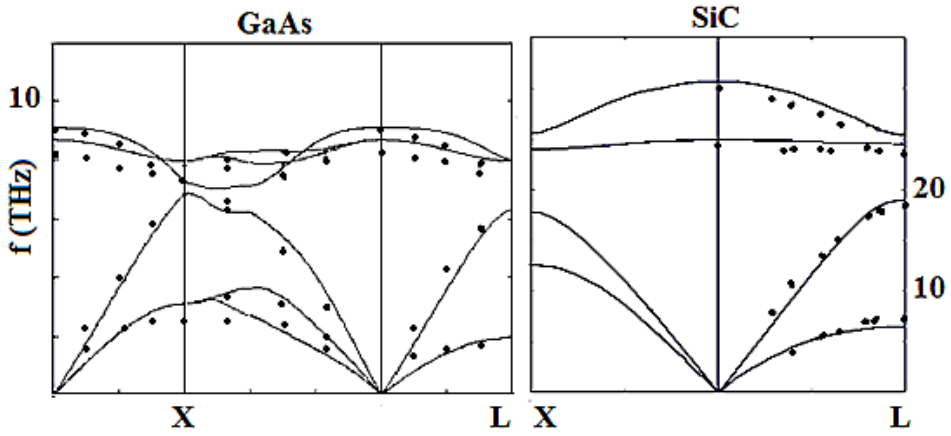

Figure 2. Phonon dispersions of GaAs and cubic SiC, in comparison to experimental data [27] and [28]. The frequency is given in THz.

Theoretical calculations and experimental data allow to obtain parameters of interatomic potential which are used in theoretical evaluation of scattering matrices [16]. Lattice thermal conductivity is then obtained in the framework of the iterative approach, introducing anharmonic parameters ε and ε' in the three-phonon scattering probabilities. Parameters ε,ε', estimated through anharmonic Grüneisen constants, are the coupling factors in the three-phonon scattering processes that we have to consider when we are evaluate the thermal resistance to phononic transport [16]. In a three-phonon scattering process, two phonons disappear to give an emerging phonon or a phonon decays in two others. Theoretical approach [16] to three-phonon processes assumes a phonon wave-vector q belonging to a true lattice Brillouin Zone. Momentum conservation is then rigorously treated, in normal and umklapp processes.

To obtain thermal conductivity, the phonon Boltzmann equation is linearized with respect to phonon distribution, which is not the equilibrium one, due to presence of thermal gradients. Introducing a deviation function $\psi_Q = \psi_{\mathbf{q}p}$ (Q indicates wave-vector and polarization q, p), proportional to the difference between perturbed $n_{\mathbf{q}p}$ and unperturbed $n_Q^0 = n^0{}_{\mathbf{q}p}$ phonon distributions, linearized Boltzmann equation for a solid subjected to a thermal gradient ∇T can be assumed as in Ziman's approach, in the form [29]:

$$\frac{\partial n_Q^0}{\partial T}\vec{v}_Q \cdot \nabla T = \sum_{Q'Q''} K^-_{QQ'Q''}\left\{\psi_{Q''}+\psi_{Q'}-\psi_Q\right\} + \sum_{Q'Q''} K^+_{QQ'Q''}\left\{\psi_{Q''}-\psi_{Q'}-\psi_Q\right\} + \sum_{Q'} D_{QQ'}\left\{\psi_{Q'}-\psi_Q\right\} + B_Q\psi_Q \tag{1}$$

The 1-st and 2-nd terms on right hand side describe three-phonon scattering processes and the 3-rd term elastic scatterings due to impurities (point defects). The last term provides a phenomenological description of boundary scattering as a relaxation time. By $\boldsymbol{v}_Q$ the phonon group velocity $(\partial\omega_Q/\partial q) = (\partial\omega_{\mathbf{q}p}/\partial q)$ is denoted. Here we will consider only point defects, however other defects such as dislocations, grain boundaries, stacking faults could be introduced. An iterative procedure then solves Boltzmann equation [16]. Let us call:

$$\psi_Q^{(o)} = A_Q / G_Q \tag{2}$$

with

$$A_Q = \frac{\partial n_Q^0}{\partial T}\vec{v}_Q \cdot \nabla T \tag{3}$$

and

$$G_Q = \sum_{Q'Q''} K^-_{QQ'Q''} + \sum_{Q'Q''} K^+_{QQ'Q''} + \sum_{Q'} D_{QQ'} + B_Q \tag{4}$$

The recursive relation giving phonon deviation function is the following (n is the recursive index):

$$\psi_Q^{(n)} = \psi_Q^{(o)} + \frac{1}{G_Q}\left[\sum_{Q'Q''} K^-_{QQ'Q''}\left\{\psi_{Q''}^{(n-1)} + \psi_{Q'}^{(n-1)}\right\} + \sum_{Q'Q''} K^+_{QQ'Q''}\left\{\psi_{Q''}^{(n-1)} - \psi_{Q'}^{(n-1)}\right\}\right] \tag{5}$$

as in Ref.16. Once n_Q is known, heat current density U is evaluated, and from the U_i, *i-th* component of heat current U with respect to a Cartesian frame, tensor k_{ij} representative of thermal conductivity in *i*- direction can be immediately obtained.

For what concerns the so-called point defects, such as impurity atoms, substituted for the atoms of base crystal, being a point defect means a mass difference in lattice positions where defect is placed, giving an elastic scattering from a phonon *qp* into a phonon *q'p'*. Due to ΔM mass difference between regular site and defect, the kinetic energy of lattice site is changed. If the point defect is a different isotope of the same element, only mass change has to be considered [16].

4. Thermal conductivities. Natural isotope composition of materials acts on thermal transport reducing thermal conductivity. Gallium arsenide is a semiconductor material that, if it obtained by natural gallium, has 60.11% in ^{69}Ga and 39.89% in ^{71}Ga, whereas arsenide is a monoisotopic element. Since thermal conductivity in GaAs is three time smaller than in silicon, one can detect if it is possible to increase thermal transport with an enrichment of a gallium isotope. Experimental data have been obtained at the Kurchatov Institute in Moscow crystals of GaAs with an almost single ^{71}Ga isotope composition [30]. Crystals are characterized by single grains of 2-4 mm in cross-section up to 15 mm in the direction of the crystal growth. Thermal conductivities were measured by means of the standard steady-state longitudinal method in a 2.5x2.5x22. mm^3 samples. These experimental data are the first published data for isotope pure GaAs sample: some of these experimental data are reported in Table 2. Comparison between experimental data of enriched and natural samples gives a 6% increase in thermal conductivity at 250 K and a 15% increase at 100 K.

Table 2. Thermal conductivity (in W cm^{-1} K^{-1}) of GaAs, enriched and natural

Temperature (Kelvin)	GaAs enriched Exp.	GaAs natural Exp.	%	GaAs enriched Theor.	GaAs natural Theor.	%
100	2.30	1.97	15	2.36	1.93	22
150	1.10	1.00	12	1.23	1.05	17
200	0.76	0.70	9	0.80	0.71	13
250	0.56	0.53	6	0.62	0.57	9

Theoretical calculations done with iterative technique are shown in Table 2 for comparison: the agreement with the experimental data is good. But, it is necessary to note that the isotope effect turns out to be more relevant in theoretical calculations. It means that other scattering mechanisms could be present in the sample, interfering with isotope effect. In Ref.30, it is in fact reported the presence of impurities coming from arsenic element.

Another scattering mechanism on the phonon transport can come from point defects as antisites, where a Ga atom is substituted by an As atom or vice-versa. Antisites produce a strong reduction of *k*, as it is obtained in the calculation of the thermal conductivity in cubic SiC. Theoretical calculations are also in agreement with estimations of Daly et al. [31], obtained with molecular dynamics.

Thermal conductivity of cubic SiC must consider the presence of antisites, where a Si atom is substituted by a *C* atom or vice-versa, as point-defect phonon scattering mechanism. Antisites produce a strong reduction of thermal conductivity, in agreement with MD simulations and with experimental observations in irradiated specimens [32-34]. The thermal conductivity of pure cubic SiC , with a scattering mechanism produced by the presence of microcrystallites, had been discussed in [17]. Here, let us pinpoint the presence of antisites. A concentration of 0.5% point defects was considered. In Table 3, the result of calculations is shown in comparison with data obtained by means of the MD simulations [34]. In the table, thermal conductivity *k* for a perfect crystals is also shown. Antisites produce a strong reduction of *k* (in agreement with data obtained by Ju Li et al. [34] with MD simulation and with experimental observations in irradiated specimens [35,36]).

Table 3. Thermal conductivity (in W cm^{-1} K^{-1}) of SiC

Temperature (Kelvin)	Thermal conductivity k perfect lattice (iterative approach) in W cm^{-1} K^{-1}	Thermal conductivity with antisite disorder (iterative approach) in W cm^{-1} K^{-1}	Thermal conductivity with antisite disorder (Molecular Dynamics) in W cm^{-1} K^{-1}
450	2.6	0.5	0.30
600	1.7	0.45	0.30
900	1.3	0.35	0.32
2000	0.5	0.30	0.30

Let us stress that the presence of grain boundaries strongly reduces the thermal conductivity of at least 20% at room temperature (from 4.2 to 3.5 *W* cm^{-1} K^{-1} at 300 *K*) [17]. But an antisite disorder is quite strong in reducing thermal conductivity: it reduces the thermal transport of one order of magnitude when 0.5% of the lattice sites are involved as antisites.

Summary. In the previously proposed approach to the evaluation of thermal conductivity, we have used a pair potential the parameters of which are estimated from fitting phononic dispersion curves and Grüneisen data. Static and high frequency dielectric constants are involved for determining the gap between acoustic and optical phonon dispersion. Since phonon dispersions, Grüneisen and dielectric constant are often available from scientific literature, this approach can be easily applied to other zincblende crystals. The proposed method for evaluating thermal conductivity is better that those using the relaxation time approximation [37], because it is based on a rigorous approach to the phonon scattering. Of course, calculations from first principles or molecular dynamics are possible too. However, the method here proposed is more intuitive, being based on parameters which can be easily evaluated from the measurements of macroscopic physical quantities.

References

[1] G.A. Slack, R.A. Tanzilli, R.O. Pohl and J.W. Vandersande (1987). The Intrinsic Thermal Conductivity of AlN. J. Phys. Chem. Solids, Volume 48, Page 641.
[2] K. Watari and S.L. Shinde (2001). High Thermal Conductivity Materials. MRS Bulletin, Volume 26, Issue 6, Page 440.
[3] R. Maboudian, C. Carraro, D.G. Senesky and C.S. Roper (2013). Advances in Silicon Carbide Science and Technology at the Micro- and Nanoscales. Journal of Vacuum Science & Technology A, Volume 31, Issue 5, Page 050805.
[4] S.E. Saddow (2012). Silicon Carbide Biotechnology: A Biocompatible Semiconductor for Advanced Biomedical Devices and Applications. Elsevier.
[5] Ming Ruan, Yike Hu, Zelei Guo, Rui Dong, J. Palmer, J. Hankinson, C. Berger and W.A. De Heer (2012). Epitaxial Graphene on Silicon Carbide: Introduction to Structured Graphene. MRS Bulletin, Volume 37, Issue 12, Page 1138.
[6] Insaco Inc, Quakertown Pennsylvania, 2015, http://www.insaco.com/ materials/carbides/cvd-silicon-carbide
[7] Insaco Inc, http://www.insaco.com/ materials/carbides/silicon-carbide-sintered
[8] A.C. Sparavigna (2012). Measuring the Thermal Diffusivity in a Student Laboratory, Engineering, Volume 4, Issue 5, Page 266.
[9] K.J. Kim, Y.W. Kim, K.Y. Lim, T. Nishimura and E. Narimatsu (2015). Electrical and Thermal Properties of SiC–AlN Ceramics Without Sintering Additives. Journal of the European Ceramic Society, Volume 35, Issue 10, Page 2715.
[10] Z. Su, J.A. Malen, J.P. Freedman, R.F. Davis, J.H. Leach and E.A. Preble (2013). Dependence of Thermal Conductivities of the AlN Film in the LED Architecture on Surface Roughness and Lattice Mismatch. ASME Paper No. HT2013-17116.
[11] A.C. Sparavigna (2014). Light-Emitting Diodes in the Solid-State Lighting Systems. International Journal of Sciences, Volume 3, Issue 11, Page 9.

[12] T.R. Anthony, W.F. Banholzer, J.F. Fleischer, L. Wei, P.K. Kuo, R.L. Thomas and R.W. Pryor (1990). Thermal Diffusivity of Isotopically Enriched ^{12}C diamond. Physical Review B, Volume 42, Issue 2, Page 1104.
[13] T. Ruf, R. Henn, M. Asen-Palmer, E. Gmelin, M.Cardona, H.-J. Pohl, G. Devyatych and P. Sennikov (2000). Thermal Conductivity of Isotopically Enriched Silicon, Solid State Commun., Volume 115, Page 243.
[14] A. Sparavigna (2002). Influence of Isotope Scattering on the Thermal Conductivity of Diamond. Physical Review B, Volume 65, Issue 6, Page 064305.
[15] M. Asen-Palmer, K. Bartkowski, E. Gmelin, M. Cardona, A.P. Zhernov, A.V. Inyushkin, A.N. Taldenkov, V.I. Ozhogin, K.M. Itoh and E.E. Haller (1997). Thermal Conductivity of Germanium Crystals with Different Isotopic Compositions. Physical Review B, Volume 56, Issue 15, Page 9431.
[16] M. Omini and A. Sparavigna (1997). Heat Transport in Dielectric Solids with Diamond Structure. Nuovo Cim. D, Volume 19, Issue 10, Page 1537.
[17] A. Sparavigna (2002). Lattice Thermal Conductivity in Cubic Silicon Carbide. Physical Review B, Volume 66, Issue 17, Page 174301.
[18] R.S. Mulik and P.M. Pandey (2011). Ultrasonic Assisted Magnetic Abrasive Finishing of Hardened AISI 52100 Steel Using Unbonded SiC Abrasives. International Journal of Refractory Metals and Hard Materials, Volume 29, Issue 1, Page 68.
[19] H.Y. Xu, Q. Yang, X.L. Wang, X.Y. Liu, Y.L. Zhao, C.Z. Li and H. Watanabe (2015). Improving Interface Quality of 4H-SiC MOS Devices with High Temperature Oxidation Process in Mass Produce Furnace. Materials Science Forum, Volume 821, Page 484.
[20] M. Gad-el-Hak (2005). MEMS: Design and Fabrication, CRC Press.
[21] Data available from D.W. Palmer, www.semiconductors.co.uk, 2014.
[22] R.S. Okojie, D. Lukco, V. Nguyen and E. Savrun (2015). 4H-SiC Piezoresistive Pressure Sensors at 800° C With Observed Sensitivity Recovery. Electron Device Letters, IEEE, Volume 36, Issue 2, Page 174.
[23] R.S. Okojie, R.D. Meredith, C.T. Chang and E. Savrun (2014). High Temperature Dynamic Pressure Measurements Using Silicon Carbide Pressure Sensors. IMAPS High Temperature Electron. Conf., Albuquerque, NM, USA, Page 47.
[24] T.T.H. Eng, S.C. Kan and G.K.L. Wong (1995). Surface-Micromachined Epitaxial Silicon Cantilevers as Movable Optical Waveguides on Silicon-on-Insulator Substrates. Sensors and Actuators A, Volume 49, Issue 1, Page 109.
[25] M. Born and K. Huang (1954). Dynamical Theory of Crystal Lattices. Clarendon.
[26] Data available from www.ioffe.rssi.ru/SVA/NSM/Semicond/GaAs/basic.html
[27] D. Strauch and B. Dorner (1990). Phonon Dispersion in GaAs. Journal of Physics: Condensed Matter, Volume 2, Issue 6, Page 1457.
[28] D.W. Feldman, J.H. Parker Jr., W.J. Choyke, and Lyle Patrick (1968). Phonon Dispersion Curves by Raman Scattering in SiC, Polytypes 3C, 4H, 6H, 15R, and 21R. Phys. Rev., Volume 173, Page 787.
[29] J.M. Ziman (1960). Electrons and Phonons: the Theory of Transport Phenomena in Solids, Clarendon.
[30] A.V. Inyushkin, A.N. Taldenkov, A.Yu. Yakubovsky, A.V. Markov, L. Moreno-Garsia and B.N. Sharonov (2003). Thermal Conductivity of Isotopically Enriched 71GaAs Crystal. Semiconductor science and technology, Volume 18, Issue 7, Page 685.
[31] B.C. Daly, H.J. Maris, K. Imamura and S. Tamura (2002). Molecular Dynamics Calculation of the Thermal Conductivity of Superlattices. Physical Review B, Volume 66, Issue 2, Page 024301.
[32] R.E. Taylor, H. Groot and J. Ferrier (1993). Thermophysical Properties of CVD SiC. TRPL 1336, Thermophysical Properties Research Laboratory Report, School of Mechanical Enginnering, Purdue University, November 1993.
[33] D.J. Senor, G.E. Youngblood, C.E. Moore, D.J. Trimble, G.A. Newsome and J.J. Woods

(1996). Effects of Neutron Irradiation on Thermal Conductivity of SiC-based Composites and Monolithic Ceramics. Fusion Technology, Volume 30, Issue 3, Page 943.
[34] Ju Li, L. Porter and S. Yip (1998). Atomistic Modeling of Finite-Temperature Properties of Crystalline β-SiC: II. Thermal Conductivity and Effects of Point Defects. Journal of Nuclear Materials, Volume 255, Issue 2, Page 139.
[35] M. Rohde (1991). Reduction of the Thermal Conductivity of SiC by Radiation Damage. Journal of Nuclear Materials, Volume 182, Page 87.
[36] R.J. Price (1973). Neutron Irradiation-Induced Voids in Beta Silicon Carbide. Journal of Nuclear Materials, Volume 46, Issue 3, Page 268.
[37] A.C. Sparavigna and S. Galli (2012). L'equazione di Boltzmann per la conducibilità termica fononica nell'approssimazione dei tempi di rilassamento, Lulu Enterprises, Raleigh, NC.